Crystallization of struvite in the presence of calcium ions: Change in reaction rate, morphology and chemical composition

by Dyah Suci Perwitasari

Crystallization of struvite in the presence of calcium ions: Change in reaction rate, morphology and chemical composition

D. S. Perwitasari, S. Muryanto, J. Jamari & A. P. Bayuseno |

Published online: 20 Mar 2022.

Submit your article to this journal 🖉

View related articles 🗗

View Crossmark data 🗗

*Corresponding author: A. P. Bayuseno, Centre for Waste Management, Departme 61 Mechanical Engineering, Diponegoro University, Tembalang Campus, Semarang 50275, Indonesia
E-mail: apbayuseno@lecturer.undip.ac.id

CHEMICAL ENGINEERING | RESEARCH ARTICLE

Crystallization of struvite in the presence of calcium ions: Change in reaction rate, morphology and chemical composition

D. S. Perwitasari[1], S. Muryanto[2], J. Jamari[3] and A. P. Bayuseno*

Abstract: Ammonium, phosphorus, and potassium from wastewater treatment with a coexisting ion of calcium may be recovered simultaneously through struvite and struvite-(K) crystallization. This paper presents the quantitative assessment of the impact of calcium ions on the kinetics and crystallization of those crystals. Initial solutions containing dose levels of Ca^{2+} ion and pH 9 were set up for experiments in a stirred laboratory crystallization at ambient temperature. According to the pH reduction data, the observed precipitation kinetics followed in two steps; the first step (0–3 min) and the second step (3–60 min) in which linear regression analysis of both kinetic data fit with first-order rate constants. In the absence of calcium, the computed kinetic constants are respectively 2.568 h^{-1} for the first stage and 1.548 h^{-1} for the second stage. The kinetic rate constants followed with the increased dose of Ca (Ca/Mg > 0.5), which lengthened the crystallization of multiphase crystallization of Mg and Ca-phosphates. Accordingly, calcium had a negative effect on the morphology, purity, and quantity of the final crystalline product. This quantitative understanding of how calcium affects the crystallization of struvite and struvite-(K) reliably improves knowledge about controlling the quantity of wastewater recovery products.

ABOUT THE AUTHOR

D.S. Perwitasari received Ph.D. in Mechanical Engineering from Diponegoro University, Indonesia. The focus of her research is currently to conduct the synthesis of struvite through aqueous crystallization for the waste streams.

S. Muryanto is a Professor in the Chemical Engineering at the Department of Chemical Engineering, UNTAG University in Semarang, Indonesia. The focus of his research is to design and engineer struvite crystallization for the waste streams.

J. Jamari is a Professor in Mechanical Engineering, at Diponegoro University. Research interest covers many aspects of material design, surface treatment, including wear characterization and lubrication technology.

A. P. Bayuseno is a Professor in Material Science and Engineering at Diponegoro University, Indonesia. Research interest covers many aspects of ceramics design, applied crystallography, including materials characterization and waste processing.

PUBLIC INTEREST STATEMENT

This research paper provides insight into the biomineralization of Mg- and Ca-phosphates in wastewater streams. As compared to the Ca-phosphate-bearing minerals, struvite [$MgNH_4PO_4\cdot6H_2O$] formed during treatment of wastewater, provide the benefits of recovering N and P simultaneously by yielding fertilizer of low solubility with the slower-released rate of nutrients than other fertilizer product. However, struvite formation can be inhibited by the presence of Ca^{2+} in the solution. Our work proposed the unified approach that deals with a strategy for synthesizing struvite and struvite-(K) from the synthetic wastewater with and without calcium, and the quantitative interpretation of biomineralization products in the synthetic one. Following X-ray, and SEM analysis, it was found that struvite and struvite-(K) were highly inhibited and present in the microspheres when Ca-phosphate minerals were developed.

cogent ·· engineering

Subjects: Process Control – Chemical Engineering; Reaction Engineering; Biochemical Engineering

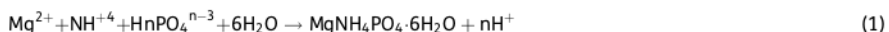**Keywords: kinetics; calcium; phosphorus and potassium recovery; struvite; struvite-(K)**

1. Introduction

Over the last decades, the industrial demand for phosphorus (P) for fertilizer production has increased dramatically along with the increase in the worldwide population, while natural phosphorus-bearing minerals are depleting rapidly (Scholz et al., 2013). On the other hand, the aquatic system in many regions worldwide is surplus insoluble phosphorus due to gray water from household liquid discharge impregnating with phosphate detergents. Such P-rich domestic effluents, along with agricultural run-off where fertilizer may have been used extensively, instigate the uncontrolled growth of algae and other aquatic plants. The unrestrained growth water florae, termed eutrophication, is unsightly as well as detrimental to environments (Li et al., 2019). Detergents containing nitrate or phosphate, fertilizer in wastewater may be found in many regions, where these substances are often discharged into an aquatic system as a result of inadequate wastewater treatment resulting in eutrophication. Therefore, extensive research to alleviate such environmental burden on the environment utilizing different techniques has been carried out.

Since phosphorus (P) is one of the vital elements required for life (Ali & Schneider, 2005; Lahav et al., 2013), the techniques capable of getting rid of eutrophication coupled with recovering the P for subsequent use are obviously more preferable, and among the various methods applied, those which could be with the intention to recover the nutrient. It is believed that simultaneous crystallization from a solution of the common three species in wastewater: Mg, N, P, termed MAP solution, yielding crystalline struvite [$MgNH_4PO_4 \cdot 6H_2O$] and its variant, e.g., struvite(K) [$KMg(PO_4) \cdot 6(H_2O)$]] is promising and worth implementing (Bhuiyan, Mavinic, Koch et al., 2008a; Bouropoulos & Koutsoukos, 2000; Doyle & Parsons, 2002). This crystallization method can be used for the concurrent reclamation of ammonium, potassium, and phosphorus from the wastewater (Ali & Schneider, 2005). Accordingly, it has been proposed as a simple and realistic means of providing a long-term supply of phosphorus (Lahav et al., 2013).

Recently, much attention has been given to implementing crystallization of struvite and/or struvite-(K) for ammonium and phosphate recovery in various types of wastewater (Bhuiyan, Mavinic, Koch et al., 2008a; Bouropoulos & Koutsoukos, 2000; Doyle & Parsons, 2002), and in the hydrothermal solution (Bayuseno & Schmahl, 2018, 2020). For this reason, the crystallization of struvite and/or struvite-(K) in MAP solution (magnesium, ammonium, and phosphate) containing potassium may be performed by adding magnesium ions in a simple bath reactor. As reported, the crystallization products of struvite and struvite-(K), both are highly insoluble in water, can be used as fertilizer (Le Corre et al., 2009).

Further, the struvite crystallization from an MAP solution is commonly represented by the following equation (Doyle & Parsons, 2002):

$$Mg^{2+} + NH^{+4} + HnPO_4^{n-3} + 6H_2O \rightarrow MgNH_4PO_4 \cdot 6H_2O + nH^+ \tag{1}$$

Hence, the mineralization of struvite depends mainly on pH, and n may vary between 0, 1, and 2. Also, struvite could be crystallized from the supersaturated solution depending on the MAP molar ratio in which a molar ratio of 1:1:1 could be a favorable condition of its formation. Fundamentally, the mechanism of the crystallization of struvite is governed by a number of factors including nucleation and crystal growth, which can be controlled by physicochemical factors such as pH, mixing intensity, temperature, and impurities in the solution (Li et al., 2016; Y. Song et al., 2014). In addition, struvite crystallized from the supersaturated solution reflects the ion activity product (IAP) of Mg^{2+}, NH_4^+, and PO_4^{3-}, which has a value above its solubility product (KSP; Bayuseno & Schmahl, 2018; Doyle & Parsons, 2002). Specifically, the successful crystallization of struvite may be under the control of pH solution and

supplied by phosphate ions. Thus, the most recent study on struvite crystallization focused mainly on controlling the pH solution with the variable molar ratio Mg/P in solution chemistry (Huang et al., 2019; Shih et al., 2017; Wang et al., 2005). As previously indicated, the pH range of 8–9 and the Mg/P ratio of 1.0–1.5 have been shown to be favorable wastewater conditions for the recovery of phosphate ions (species of PO_4^{3-} and their variants dictated by the pH levels) in the form of struvite (Bhuiyan et al., 2007; Bhuiyan, Mavinic, Koch et al., 2008b; Doyle & Parsons, 2002).

Physicochemical factors affecting struvite crystallization may also relate to the chemical composition of a digestion solution, which comes from the different sources of wastewaters with dissolved foreign ions (Rahman et al., 2011,Yan & Shih, 2016). In some cases, other constituents of wastewater could be discharged from wastewater treatment plants that subsequently react with MAP ions leading to crystallization of struvite (Le Corre et al., 2009; Karabegovic et al., 2013). In some cases, different sources of wastewater clearly contain different dissolved ions (Rahman et al., 2011,Yan & Shih, 2016) hence dictating various physicochemical variables for successful crystallization of struvite (Le Corre et al., 2009; Karabegovic et al., 2013).

In general, wastewater streams, especially in dairy wastewaters are richer in calcium than magnesium, ammonium, and phosphate, and foreign ions (Cu^{2+}, Zn^{2+}, Al^{3+}, CO_3^{2-} and SO_4^{2-}; Le Corre, 2006; Le Corre et al., 2005; Sabbag et al., 2015). A number of studies have revealed that the presence of competing ions, i.e. apart from as noted above, calcium may interfere with magnesium in MAP crystallization (Wang et al., 2005), which produced a small proportion of struvite due to unexpected bearing mineral formations of Ca, such as hydroxyapatite [$Ca_5(PO_4)_3OH$], whitlockite [TCP, $Ca_3(PO_4)_2$], octacalcic phosphate [OCP, $Ca_8(HPO_4)_2(PO_4)_4\cdot5H_2O$] and monenite (DCP, $CaHPC_4$; Bayuseno & Schmahl, 2020; Çelen et al., 2007; Hao et al., 2013).

It is common to estimate the purity of struvite as the ratio of NH_4/PO_4 in the precipitates. In regard this estimation, it has long been observed that a clear trend in the decreasing of struvite purity was seen when higher Ca/Mg ratios were employed (Wang et al., 2005). Using synthetic wastewater mimicking the effluents of anaerobic digestion lagoons treating piggery wastes, Wang et al. (2005) reported a gradual decrease in struvite purity from 85% down to a mere 38% when the Ca/Mg were increased four times, i.e. from 0.5:2 to 2:2. With such a decrease it can be assumed that Ca is the main interfering cation during the precipitation of struvite capable of replacing the NH_4 ions in the process.

Compared with calcium phosphate crystallization, MAP one involves the process of recovering ammonium and phosphate on which there is no need for injection of seed crystals. The crystallization method is also simply used to recover phosphates (Liu et al., 2013; song, Donnert et al., 2007; Song, Yuan et al., 2007). MAP precipitation can also be applied as a slow-release, long-acting fertilizer (Liu et al., 2013). Because of its favorable technique, MAP crystallization could be used for phosphate recovery from pig sewage (Capdevielle et al., 2013; Crutchik & Garrido, 2011).

Conversely, high concentrations of Ca^{2+} in the MAP solution could increase phosphorus removal efficiency from 58% to 92% (Huang & Liu, 2014; Lee et al., 2013; Pastor et al., 2008). This substantial gain in the phosphorus removal efficiency occurred favorably at Ca/Mg molar ratios above 2, while ratios below 0.5 would not impact the crystallization of struvite (Desmidt et al., 2013). The impact of calcium on struvite crystallization was also observed at low concentrations of magnesium and ammonium in the solution, resulting in the formation of other undesirable minerals and a change in struvite morphology (Le Corre et al., 2005).

Currently, the impact of varying Ca/Mg ratio on the struvite crystallization in the wastewater has become an intensive study focusing on morphology and purity of the product, whilst the use of simple reactors with the batch system for phosphate recovery by adding magnesium reagent on the wastewater is commonly implemented (Dalecha et al., 2014). In particular, batch crystallization offers numerous advantages in the laboratory and industrial applications. The laboratory crystallizer also assists in characterizing the crystallization kinetics and crystal size distribution (RDS) and determining the impacts

of process conditions on these kinetics and CSDs. Therefore, wastewater treatment in the batch system is seen as a good deal more economical with low production capacities of approximately 1 m^3 of product per day or less. In addition, batch crystallization offers an advantage with the ability to produce uniform particle size.

However, the quantification of precipitates containing struvite and struvite-(K) from a batch crystallization process as indicators of economic viability has not been specifically investigated. The corresponding data of the mineral compositions of solid products precipitated from the aqueous solution at varying Ca/Mg ratios and their effects of competition between Ca-P and Mg-P, including their crystallization kinetics, were nevertheless limited. Consequently, this batch crystallization study with synthetic wastewater was designed to study the influence of Ca2+ ions on the crystallization of precipitates based on the analysis of the analytical tool. In addition, the Mg and Ca-competitions for the recovery of phosphates from synthetic wastewater as potential phosphate minerals were studied using XRPD (X-ray powder diffraction) and SEM (scanning electron microscopy) analyses combined with kinetic data. The predicted limit value of the Ca/Mg molar ratio controlling crystallization in the synthetic wastewater would be helpful in managing the purity and quality of struvite and struvite-(K) in the future.

2. Experimental

2.1. Batch precipitation experiments

The struvite crystallization experiments were carried out using an agitated laboratory glass beaker of 200 ml volume. Anhydrous magnesium chloride ($MgCl_2$) and ammonium dihydrogen phosphate ($NH_4H_2PO_4$) crystals (Merck, AR grades) were used for the struvite crystallization providing ions: Mg^{2+}, NH_4^+, and PO_4^{3-} necessary for the reaction. Moreover, a stock solution concentration of 0.17 M each was prepared from those chloride and phosphate powder crystals, which were analytically weighed (WANT Balance, FA-N Series, 0.0001 g) and then diluted separately with distilled water. The dissolution was carried out using standard laboratory glassware (graduated cylinders, volumetric flasks, and other glass apparatus of various sizes). In view of the pH solution being affected by absorbing CO_2 from the air into the solution due to long-standing distilled water, boiling the distilled water was necessary and left to cool in a closed container prior to the dissolution. Next, a pH of 9.00 in the mixed solution was set up by drop-wise addition of 0.2 N KOH (Bhuiyan et al., 2007; Bhuiyan, Mavinic, Koch et al., 2008b; Doyle & Parsons, 2002). The pH adjustment was required for struvite crystallization that occurs only in basic conditions. In the experiment, the chemical compositions of crystal-forming solutions are presented in Table 1.

In the individual crystallization run, 175.5 mM $MgCl_2$ and 175.5 mM $NH_4H_2PO_4$ solutions were dissolved in 50 ml each of a 200 ml-glass beaker. The beaker containing mixed solution was constantly stirred to ensure that the crystallizing solution was homogeneous. An impeller speed of 200 rpm was found to be appropriate for the homogeneity of the solution without breaking the crystals. The pH solution was continuously read using a pH meter (METTLER Toledo-portable pH

No	Ion (mM)	Mg:NH$_4$:PO$_4$ (1:1:1)	Ca:Mg (0.5:1)	Ca: Mg (1:1)	Ca:Mg (2:1)
1.	Mg	175.5	175.5	175.5	175.5
2.	NH$_4$	175.5	175.5	175.5	175.5
3.	PO$_4$	175.5	175.5	175.5	175.5
4.	K	500	500	500	500
5.	Ca	0; 0.01; 0.1; 0.2	87.75	175.5	351
6.	Cl	351	351	351	351

Table 1. The chemical composition of the crystallizing solution

meter), which was immersed in the mix solution for about 80 min. Eventually, the precipitates were quickly filtered by filter membrane (Whatman®—WHA1001325—grade 1) and air-dried in secure place. The precipitating solids were kept for subsequent material characterizations, i.e. scanning electron microscope (SEM) coupled with energy dispersive spectroscopy (EDS), and X-ray powder diffraction (XRPD) method.

2.2. Kinetic analysis

As stated previously, the current crystallization was focused on the influence of impurity on crystallization, i.e. calcium ions since Ca^{2+} is one of the major cations present in wastewater. It was previously reported that the presence of impurities, i.e. even in ppm quantities, might influence significantly on the crystallization (Bayuseno et al., 2020; Muryanto & Bayuseno, 2014). For this experiment, powder crystals of $CaCl_2 \cdot 2H_2O$ were dissolved in distilled water and subsequently diluted into the $MgCl_2$ solution in predetermined concentrations (1, 10, 20 ppm and, Ca: Mg ratios of 0.5, 1 and 2). The experiment was carried out at ambient temperature to make sure that no ammonia/nitrogen component evaporated from the solution. In fact, many WWTP (wastewater treatment plants) normally work at ambient conditions (Shih et al., 2017). Correspondingly, experimental runs were performed to predict the length of the crystallization run and to validate the reproducibility of the measurements. Therefore, it was then decided that the run was done in triplicate for each measurement.

In the present study, the struvite growth rate was estimated by observing the pH changes as the crystallization progressed; while the pH drop corresponded to the decrease in $[Mg^{2+}]$ as described in Equation (2). As shown in Equation (1; see Introduction), the rate of struvite crystallization can be presented as either the rate of reduction of $[Mg^{2+}]$ or the rate of increase in hydrogen ion concentration, $[H^+]$. Mathematically, the relationship is expressed (Muryanto & Bayuseno, 2014) as:

$$\ln(C - Ceq) = -kt + \ln(C - Co) \tag{2}$$

where:

C = $[Mg^{2+}]$ at any time t (molar)

Ceq = $[Mg^{2+}]$ at equilibrium (molar)

Co = initial $[Mg^{2+}]$ at time zero (t = 0) (molar)

k = kinetic parameter (h^{-1})

t = precipitation time (min)

In batch experiments, a digital pH meter recorded the pH continuously during precipitation. In the kinetic analysis, a pH solution was seen over time (Bayuseno et al., 2020; Muryanto & Bayuseno, 2014). After 80 minutes of testing, the stirrer was turned off, then the solution was separated by 0.45 μm filters. Eventually, the precipitates were cleaned with deionized water to remove impurities from the crystal surfaces. In this study, only chlorides and alkali ions could be released during scrubbing. The precipitate slurries were then dried at room temperature for 48 hours, and stored in a small plastic container for later characterization.

2.3. Mineralogical phase characterization

The obtained precipitating solid was dried and then subjected to the X-ray powder diffraction (XRPD) measurements. Initially, the dried solid was ground to provide a grain size of less than 75 μm and later mounted in the Aluminum-XRPD sample holder. The XRPD data were collected by Bragg Brentano (Philips 1830/40) X-ray diffractometer at room temperature using Cu Kα radiation,

where the fixed measurement parameters (5–85° 2θ; 0.02° steps; 15s/steps) were employed. The identified phases in the samples were acquired by the diffraction line-matching program (Match software), whilst the resulting phases were then verified by the qualitative and quantitative Rietveld method (Fullproof-2k, version 3.30; Rodriguez-Carvajal, 2005; Wiles & Young, 1981; Young, 1993). The abundant crystalline phase (weight. %) in the sample was calculated using refined results of the unit cell parameters and the scale factor (Hill & Howard, 1987). Detailed Rietveld refining procedures were established according to the methodology reported previously (Bayuseno & Schmahl, 2015; Mahieux et al., 2010).
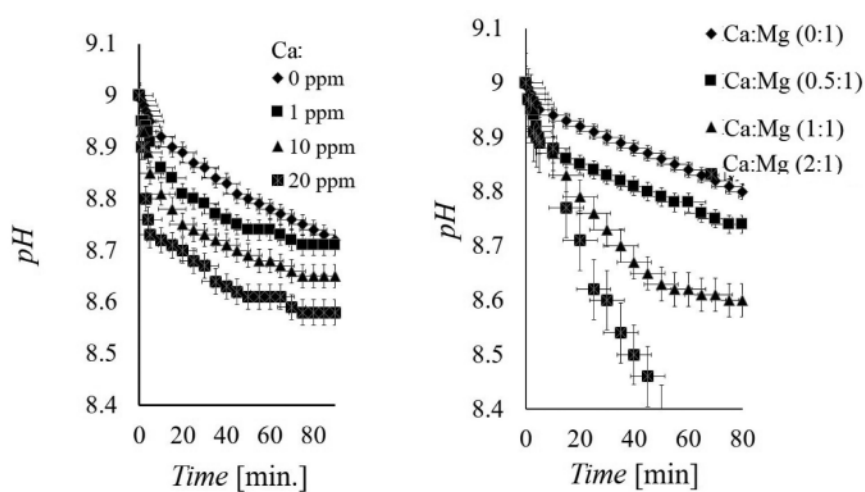
Further, the ground powder samples were mounted with glue on the Al-sample holder surface, and coated with carbon for the morphological analysis by SEM (JEOL JSM 5200), while the composition of the chemical element was determined by the EDX system.

3. Results and discussion
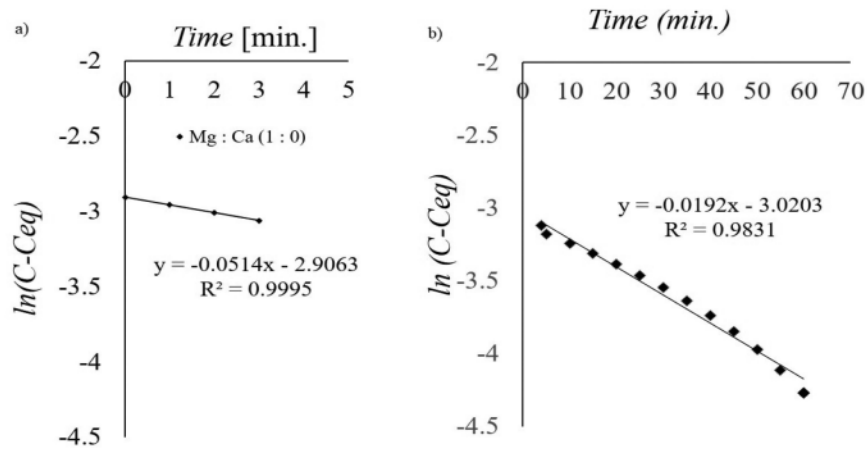
3.1. Precipitation kinetics

The precipitation kinetics was calculated based on the reduction of the Mg^{2+} in the solution by manipulating the decrease in pH values as shown by the pH meter readings (Muryanto & Bayuseno, 2014). The manipulation was fairly simple in that during the process of the precipitation of struvite it was demonstrated that $[Mg^{2+}] = [H^+]$ throughout in the study (Bayuseno et al., 2020; Nelson et al., 2003; Quintana et al., 2005). In fact, struvite precipitation is mainly under control by pH, initial relative MAP concentrations, and other coexisting cation of Ca^{2+}. Accordingly, pH is regarded as a key aspect to control struvite crystallization (shape, morphology, and purity). Moreover, the present kinetic experiments were relied on the change of pH that could be related to the decreased Mg^{2+} concentration at the ambient temperature and at a constant stirring speed of 200 rpm with varying Ca- concentrations. Figure 1 shows a drop in pH over time in the solution with and without variable calcium concentrations at 30 °C. In the absence of Ca^{2+}, the pH falls abruptly over the first three (3) minutes and then gradually decreases (Figure 1a-b). Just after 80 minutes, the pH solution appears to be fairly stable. During the first 3-minute period, the pH decrease corresponded to the struvite crystallization (Ali & Schneider, 2006; Darwish et al., 2017; Kofina et al., 2007; Prywer et al., 2012; Rahaman et al., 2008), whereas the second phase may concern the formation of other Mg-bearing minerals. The response rate constants were then predicted by linearly fitting the experimental data in the modified first-order kinetic model

Figure 1. The crystallization of struvite using $MgCl_2$ (175 mM) and a) added Ca^{2+}: 0, 1, 10, and 20 ppm; b) Ca/Mg ratios: 1; 0.5:1, 1:1, 2:1. Error bars are also shown.

Figure 2. Struvite crystallization of using using MgCl$_2$ (175 mM) in the absence of Ca^{2+} fitting at the first-order kinetic C = [Mg^{2+}] at time t; Ceq = [Mg^{2+}] at equilibrium, in the period of a) 0–3 minutes; b) 3–60 minutes.

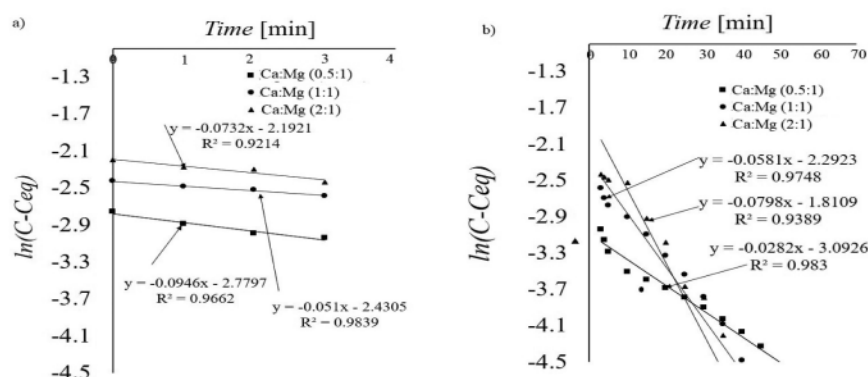| Table 2. Kinetic parameters of the crystallization. Stirring speed of 200 rpm and T = 30°C				
	The first stage (0–3 min)		The second stage (3–60 min)	
Amount of Ca^{2+}	Rate constant (h^{-1})	R^2	Rate constant (h^{-1})	R^2
0 ppm	2.568	0.9991	1.548	0.9907
1 ppm	4.074	0.8799	2.430	0.9830
10 ppm	6.684	0.9275	2.406	0.9819
20 ppm	15.33	0.9670	2.400	0.9669
Ca/Mg = 0.5:1	5.676	0.9662	1.692	0.9830
Ca/Mg = 1:1	3.060	0.9839	3.486	0.9748
Ca/Mg = 2:1	4.392	0.9214	4.788	0.9389

(Figure 2). The calculated rate constants are presented in Table 2. In the first period, this model provided an estimated rate constant of 2.568, 4.074, 6.684, 15.33 h^{-1} at Ca^{2+} concentrations of 0, 1, 10 and 20 ppm, respectively. Moreover, those results in the absence of Ca^{2+} are in reasonable agreement with those reported Nelson et al. (2003) and Rahaman et al. (2008).

In contrast, the increasing reactions to the presence of Ca were observed, in turn, inhibiting the struvite crystallization (Figures 3a, b). Here, varying rate constants (5.676, 3.060, and 4.392 h^{-1}) with respect to Ca concentration were obtained in Ca/Mg ratios of 0.5, 1, and 2, respectively (Table 2). In this regard, variable-rate constants may relate the constituent ion concentrations controlling to the supersaturation ratios of precipitated phosphate-bearing minerals. Evidently, calcium delayed the induction time of struvite crystallization for the first appearance of its crystal and interfered with the growth rate of struvite (Bouropoulos & Koutsoukos, 2000; Le Corre et al., 2005).

Regarding the accuracy for the kinetic model, the present developed model was compared with other models reported for struvite precipitation from wastewater stream in which some of the published papers had been refereed (Ali & Schneider, 2006; Le Corre, 2006; Darwish et

Figure 3. Struvite crystallization from the solution with a MAP ratio of 1:1:1 and the presence of Ca²⁺ fitting at the first-order kinetic C = [Mg²⁺] at time t; Ceq = [Mg²⁺] at equilibrium, in the period of a) 0–3 minutes; b) 3–60 minutes.

al., 2017; Kofina et al., 2007; Nelson et al., 2003; Prywer et al., 2012). Evidently, the obtained uncertainties of parameters and significant numbers in this current study were in good agreement with those reported in those papers. Accordingly, the present kinetic analysis provided accurate results that agreed very well with those of published papers for struvite crystallization in the batch system.

3.2. Purity and morphological crystal products

The crystallized products without and with calcium (0, 1, 10, and 20 ppm) were assessed qualitatively by a computerized search-match procedure of the XRPD method, relying on the powder diffraction file (PDF) from the International Centre for Diffraction Data (ICDD). As a result, most of the struvite-(K) (PDF#70-2345) and struvite (PDF#71-2089) were found, along with sylvite (PDF #73-0380). These phases identified were then validated by the Rietveld refining method as shown that the observed (Y_{Obs}) profile patterns agreed very well with calculated (Y_{calc}) profile ones (Figure 4a for crystal samples collected with 20 ppm Ca²⁺). Moreover, three phases of struvite, struvite-(K), and sylvite were confirmed to be found in the precipitation collected with increases in Ca concentrations (0 to 20 ppm) (Figure 4b). Clearly, the composition of the collected precipitate phases was not modified under the influence of these Ca²⁺ concentrations. As a result of the minerals formed a solid solution, precipitates can be made from a

Figure 4. (a) XRPD Rietveld refinement plot of the precipitating solid from the MAP solution (1:1:1) at initial pH 9 and coexisting Ca²⁺ cation (20 ppm). Noted: Yobs and Ycalc are observed and calculated XRPD intensities, respectively. (b) XRPD pattern of the samples precipitated from the solution with MAP molar ratio (1:1:1) and initial pH with different concentrations of Ca²⁺ (0, 1, 10 and 20 ppm). Notes: struvite (S); struvite-(K) (S(k)) and sylvite (Sv), respectively.
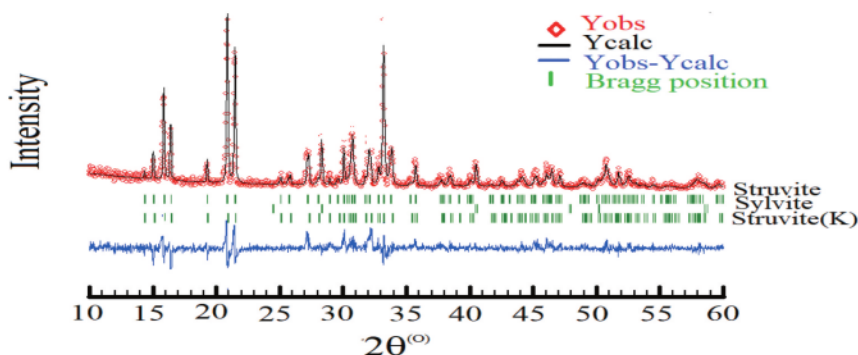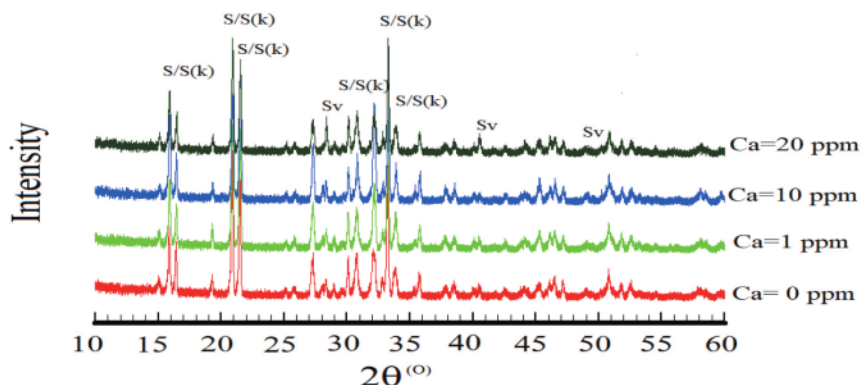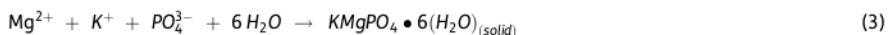
Figure 4. Continued.

mixture of any single crystal.

As shown previously (Figures 1 and 2), two stages of precipitation are suggested to occur in the solution (Ca/Mg ratio > 0.5) at the temperature of 30 $^{\circ}$C, upon which two Mg-bearing minerals would be formed during crystallization. In this regard, the pH decrease was observed in two distinct steps; in the first stage (0–3 min), the pH decreased quite sharply; but in the second stage, the pH decreased progressively (3–60 min). These steps were supported by XRPD results confirming that two crystalline phases were formed. Correspondingly, struvite-(K) was precipitated instead of struvite according to (Equation 3):

$$Mg^{2+} + K^+ + PO_4^{3-} + 6H_2O \rightarrow KMgPO_4 \bullet 6(H_2O)_{(solid)} \tag{3}$$

Hypothetically, struvite-(K) was formed because of excess KOH ions present when adjusting the pH in the MAP solution. An initial pH-9 solution with a Ca/Mg ratio higher than 0.5 was favorable for the recovery of phosphate and potassium as struvite-(K; Bouropoulos & Koutsoukos, 2000; Song, Donnert et al., 2007).

Additionally, XRPD diffractograms of precipitating solids at Ca/Mg ratios are shown in Figure 5. Each peak profile has been checked using the Rietveld refining method and linked to the standard mineral database. With Ca/Mg ratios of 1 and 2, the formation of struvite, struvite-(K), sylvite, hydroxyapatite ($Ca_5(PO_4)_3OH$), dolomite ($CaMg(CO_3)_2$), portlandite ($CaOH$), Mg-whitlockite (Ca_9Mg $(PO_4)_6PO_3OH$), newberyite ($MgPO_3OH$)•3(H_2O) could be affirmed. It may also include amorphous calcium precipitate, which could not be fully identified with the XRPD method. However, this suggestion would be later justified by the EDX analysis. When the chemistry solution has a molar ratio of Ca:Mg > 0.5:1, there is evidence of the formation of hydroxyapatite, dolomite, and portlandite associated with the presence of Ca^{2+} ions, which competes with phosphate ions in crystallization processes (Le Corre et al., 2005). As a result, the interaction of calcium with phosphate ions in wastewater systems can typically produce poorly crystallized hydroxylapatite based on the following reaction (Equation 4):

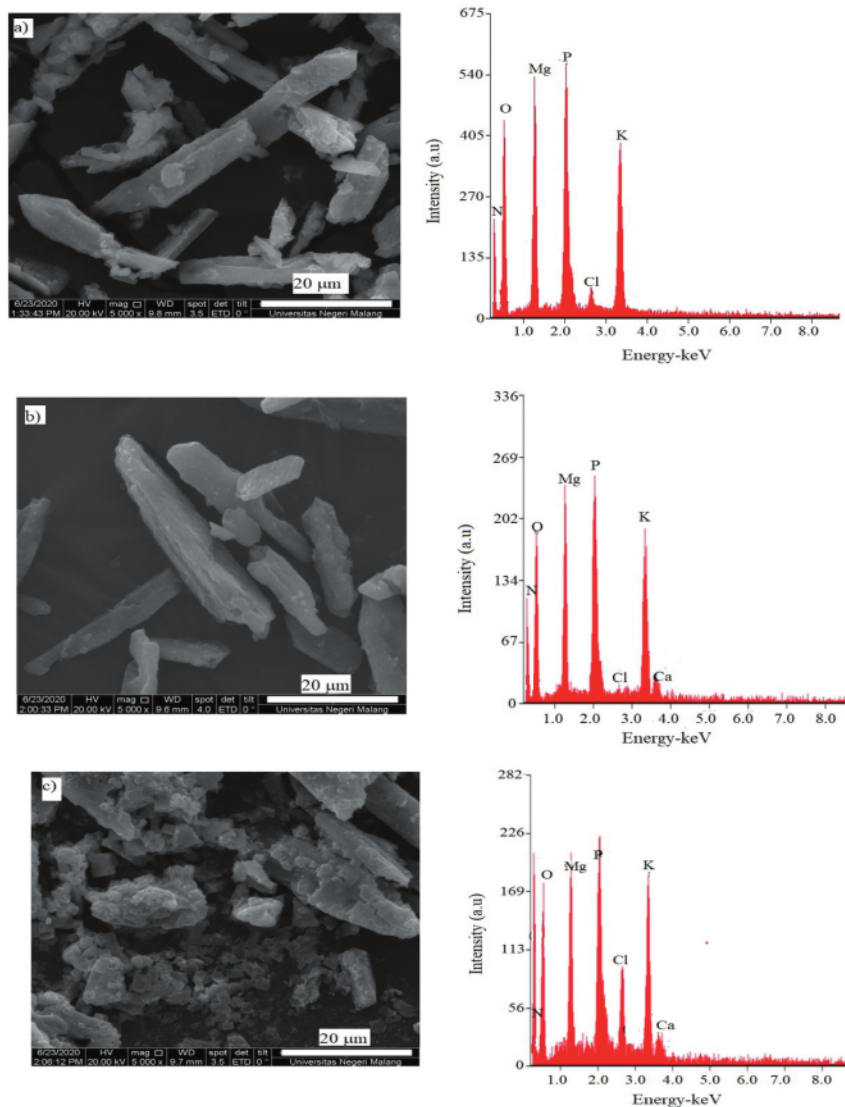$$5Ca^{2+} + 3PO_4^{3-} + H_2O \rightarrow Ca_5(PO_4)_3 + OH + H^+ \tag{4}$$

Instead, under the condition of a (Ca/Mg) ratio greater than 0.5, the presence of calcium was reported to insignificant contribution to the P removal efficiency but only influence the purity of

✳ cogent ✦ engineering

Figure 5. XRPD pattern of the samples precipitated from the solution with MAP molar ratio (1:1:1) and initial pH with different Ca/Mg ratios (0, 1, 2 and 0.5). Notes: dolomite (D); hydroxyapatite (HA); P (portlandite); struvite (S); struvite-K (S(k)); sylvite (Sv); Mg-whitlockite (Wt), respectively.

struvite crystals as confirmed by the XRPD analysis. In some cases, the struvite-like crystals might be enclosed with an amorphous phase, probably amorphous hydroxylapatite (Le Corre et al., 2005).

Other calcium effects on the development of crystal morphology were also examined with SEM-EDX. In the absence of calcium, struvite crystals with needle morphology (40 μm long and 10 μm wide) were evident in the SEM images (Figure 6a). Apparently, the growth of the struvite crystal appeared to extend along the longitudinal axis. Additionally, struvite-(K) with an elongated rectangular bar-shaped morphology could be observed. The corresponding EDX spectrum confirmed the distinct peaks associated with K^+, Mg^{2+}, O^{2-}, and P^{3-} (in % mass), for constituent minerals of struvite and struvite-(K). It was noted here that the carbon peak could be observed to relate the carbon-coated on the surface of the sample for the analysis. Instead, at a low calcium concentration (10 and 20 ppm), the crystals of the struvite and struvite-(K) are shown to be attached with a precipitate (Figure 6b-c), suggesting that no other phase precipitates on those crystal surfaces interacted with their crystallization and the less amount of Ca^{2+} could be absorbed on the surface of those crystals.

The EDX mapping analysis was afterward aimed at a specific area localized on the SEM micrographs of specimens with a coexisting cation of Ca^{2+} for the molar ratio Ca/Mg more than about 0.5. Their spectra and the specific distribution mapping of elements were presented in Figures 7a, b and c, respectively. Under the Ca/Mg ratio of 1/2 or above, as confirmed from SEM-EDX analysis, other phases might be precipitated other than struvite and struvite-(K) crystals, while cation of Ca^{2+} made the interaction with their formation through the absorption of Ca^{2+} on the surface of both crystals. This condition proposed that the evolution of the struvite and struvite-(K) crystals appeared to be inhibited and would have formed an amorphous material. For samples with an Ca/Mg ratio of 1 or greater (Figure 7b-c), EDX analysis also supported earlier XRPD findings confirming that precipitates formed in this work may include both amorphous and crystalline calcium phosphate. Additionally, the amorphous phase formed on the precipitating solid could be deduced from the multitude of background noise in the XRPD diagrams. In Figure 5 for the sample with the Ca/Mg ratio > 0.5, the XRPD diffractogram displays the background noise, while the struvite peaks are always identifiable. Likewise, the XRPD pattern for the samples is illustrated in Figure 5, which has provided evidence of decreased purity of struvite with the evolution of Ca phosphate minerals into amorphous or crystalline forms (Le Corre et al., 2005).

According to SEM observations (Figure 7a), some needle-like morphology for struvite still remained, but most were aggregated with irregular crystal sizes and shapes, which are similar

Figure 6. Impact of growing amount cation of Ca²⁺ on struvite crystal morphology and purity. SEM micrograph and their respective EDX spectrum for MAP precipitation (molar ratio of 1:1:1) added by Ca2 + cations of a) 0 ppm; b) 10 ppm; c) 20 ppm.
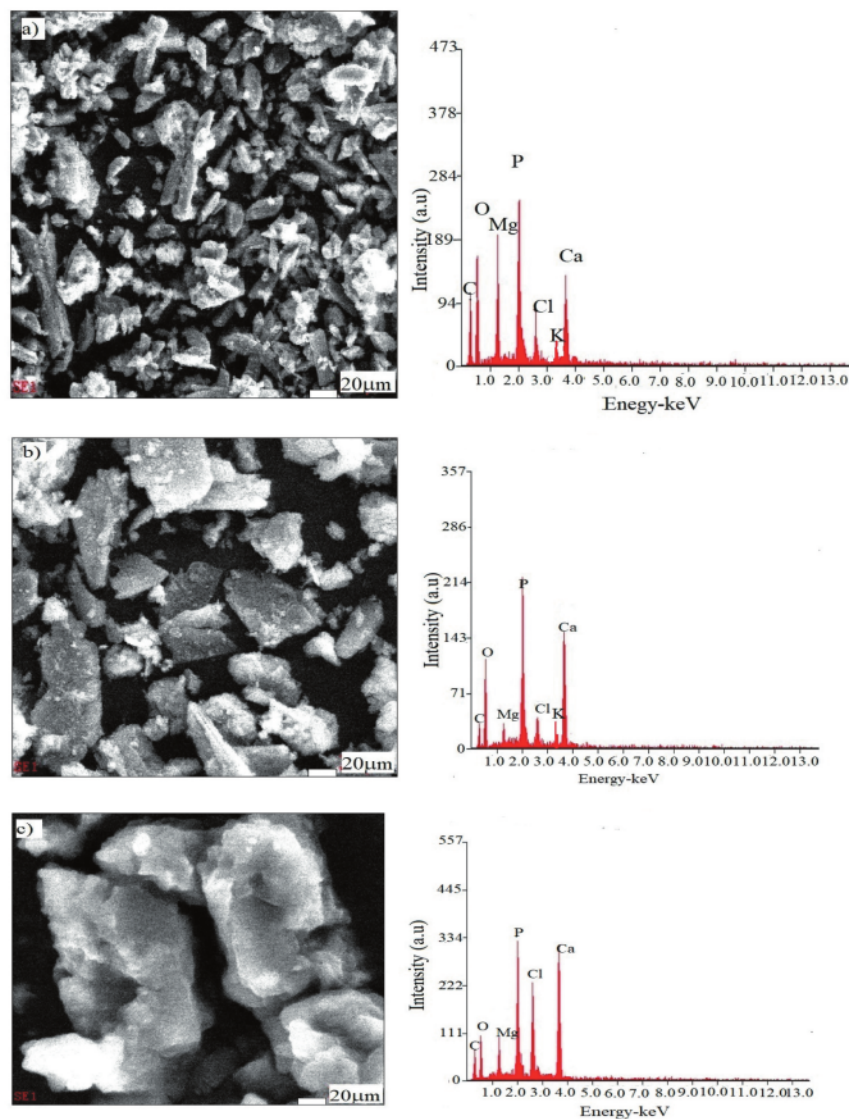

findings reported previously (Le Corre et al., 2005; Li et al., 2016). Likewise, the sample with the ratio Mg: Ca of 1:1 has some finer crystals associated with the struvite crystals observed. However, in the sample at the Ca/Mg ratio of 2:1, the needle morphology had disappeared and had been replaced by an irregular morphology (Figure 7c). This can be a result of multiphase precipitation as shown in Table 3. Here, the EDX analysis also supported the formation of Ca-phosphate minerals with higher calcium content, since both EDX spectra have higher peaks of P, Ca, and O than Mg (Figure 7b, c).

Apparently, the purity of struvite and struvite-(K) was significantly controlled by the higher ratio of Ca/Mg 1:2 (Figure 6), including the ammonium content in the chemistry solution (Le Corre et al., 2005). Although Ca/Mg ratios were similarly applied in the previous study (Le Corre et al., 2005),

Figure 7. Impact of growing amounts of Ca²⁺ ions on struvite crystal morphology and purity. SEM micrographs and their respective EDX spectrum for adding Ca ion to a molar ratio of Ca: Mg of a) 0.5: 1 b) 1:1; c) 2:1.

the present study employed a concentration of ammonium in 1:1:1 for the MAP molar ratio, which is more typical of dairy wastewater (Guillen-Jimenez et al., 2000). Where ammonium and phosphate are at the same concentration in the solution, the morphology of the product can be less sensitive to changes in Ca content. However, the degree of supersaturation of magnesium, ammonium, and phosphate in struvite production may more than offset the cost of chemical treatment to reduce the Ca content, making it less economically feasible. Accordingly, one of the main areas of reflection for reducing the concentration of it becomes a consideration for further research.

Further, different treatments of wastewater containing high calcium have been proposed in terms of their basic principles, applications, costs, maintenance, and suitability (Huchzermeier & Tao, 2012).

Currently, the precipitation method has been a proven technology for wastewater with high calcium content turning calcium carbonate. Calcium carbonate precipitation has been reported to treat wastewater in anaerobic reactors, providing a cost-effective method, easy implementation, and high efficiency (Xiaoning Liu & Wang, 2019). Hence, a degree of compromise should be considered for pre-treatment by calcium carbonate precipitation, because there is a competition between quality benefits of calcium carbonate precipitation and chemically enhanced wastewater treatment for subsequent P recovery efficiency and solution pH. In this way, the proposed treatments for wastewater with high calcium may combine two methods, in which calcium carbonate precipitation would firstly, be employed, secondly, followed by struvite crystallization.

3.3. Quantitative mineralogical phase analysis of the final products

In agreement with the previous finding of the calcium effect on the struvite crystallization process (Le Corre et al., 2005; Doyle & Parsons, 2002; Wang et al., 2005), many calcium phosphate minerals were suggested to precipitate other than struvite in the MAP solution with calcium at the higher ratio of Ca/Mg of 1. Consequently, multi-minerals would precipitate leading to the reduced quantity of struvite, although recovering phosphorus from the waste stream could be very efficient and productive. While a good slow-release fertilizer reflects the morphology and purity of struvite (Rahman et al., 2026–2030, Liu et al., 2013), the amount of struvite produced could be measured in terms of the economic feasibility of the precipitation method. In the study, the mineralogical composition of precipitates was determined according to the XRPD Rietveld refinement method, and the quantitative results according to the Ca/Mg molar ratios and its solubility product constants of the identified minerals (pKsp = —$\log^{10}$Ksp) are given in Table 3. At this point, the percentage by weight (wt. %) of each phase was calculated using the refined lattice parameter of the Rietveld method. Moreover, the pKsp values were used to understand the possibility of mineral precipitation from the thermodynamic perspective, in which these values determine the dissociation compound in water in that the greater the pKsp is the more soluble the compound. Instead of sylvite, all minerals presented in Table 3 with the positive values of pKsp are considered to have a high possibility for precipitation of the solution subject to the present study.

Firstly, in the absence of Ca^{2+}, struvite (58.45 wt. %), struvite-(K) (40.21 wt. %) were major minerals found in the collected precipitates with minor sylvite (1.34 wt. %). In this regard, the lower level of ammonium and the higher level of phosphate activity affected the generation of struvite-(K) crystal (Bouropoulos & Koutsoukos, 2000; Song, Donnert et al., 2007). In fact, the proportion of struvite and struvite-(K) products was not significantly modified when the concentration of calcium was less than 20 ppm in the solution. Additionally, the pH solution of 9–10.5 is suggested for optimal phosphate and potassium recovery in struvite and struvite-(K) products (Bouropoulos & Koutsoukos, 2000; Song, Donnert et al., 2007). Nevertheless, the calcium dosage is increased to make the adverse impact becoming pronounced. An increase in calcium concentration in the solution (Ca/Mg ratio of 0.5), made three dominant Ca-bearing minerals, namely dolomite, hydroxyapatite, and portlandite formed, where hydroxyapatite is major (13.01% by weight). Conversely, the reduction in Ca-concentration is more likely to have been initiated largely by the precipitation of hydroxyapatite.

91 Also, the reduced phosphate concentration in precipitates may correspond to the formation of amorphous calcium phosphate (ACP) as previously suggested by XRPD analysis (Figure 5; Desmidt et al., 2013). When the solution chemistry was set up at a Ca/Mg ratio of 1, struvite and struvite-(K) (7.8 and 20.20 % by weight, respectively) seemed to be inhibited by the formation of newberyite and Mg-whitlockite. Apparently, newberyite crystallized relating to the interaction of magnesium and phosphorous contents in the solution, while its crystallization is usually accompanied by struvite (Abbona et al., 1988). Accordingly, the newberyite forming reaction can be interpreted as follows (Abbona & Boistelle, 1979; Kontrec et al., 2005):

cogent · engineering

Table 3. Mineralogical phase compositions of crystallization products

	Ca: 0 ppm	Ca:1 ppm	Ca:10 ppm	Ca: 20 ppm	Ca/Mg:0.5:1	Ca/Mg:1:1	Ca/Mg: 2:1	pKsp
Struvite	58.45(27)	42.30 (76)	40.18(97)	56.91(22)*	29.78(16)	7.88(46)		13.17
Struvite-(K)	40.21(91)	55.57 (71)	58.01(32)	39.78(05)	37.10(21)	20.10(80)		11.00
Sylvite	1.34 (07)	2.13 (12)	1.81(11)	3.32(12)	9.43 (17)	33.26(50)	16.85 (72)	−0.85
Hydroxyapatite					13.01 (93)	13.79(57)	70.95 (58)	54.45
Dolomite					4.28 (22)	3.94(92)	10.65 (13)	17.09
Portlandite					0.94 (29)	12.92(69)	1.55 (58)	5.18
Mg-whitlockite						3.93(10)		28.88
Newberyite					5.46 (32)	4.18(38)		5.80

*Number in the bracket represents the standard deviation of the value.

$$Mg^{+2} + HPO_2^{-4} + 3H_2O \rightarrow MgHPO_4 \bullet 3H_2O_{(solid)} \qquad (5)$$

As reported previously, newberyite could be favorably formed in the lower pH solution (pH 6; Abbona & Boistelle, 1979). In the current experiments, however, struvite might be formed earlier than newberyite, in that the crystal nuclei of struvite supposedly promoted newberyite in the formation of crystal clusters (Abbona & Boistelle, 1979). In the 1: 1 molar ratio Ca/Mg experiment, Mg-whitlockite, and hydroxyapatite could be generated with the comparable amount as confirmed by the XRPD Rietveld method (Downs & Hall-Wallace, 2003). Those calcium phosphate minerals could be simultaneously crystallized in wastewater at room temperature (Lagier & Baud, 2003), and had been evidently found in the hydrothermal solution (Bayuseno & Schmahl, 2020; Li et al., 2016).

In addition, the corresponding struvite content in calcium experiments with Ca/Mg at 2:1 had disappeared, suggesting no interaction of ammonium and phosphate under this condition (Abbona et al., 1986; Gunay et al., 2008). Unexpectedly, a relatively large amount of sylvite (9–34% by weight) was recovered from the deposits (with Ca/Mg molar ratio < 0.5) that could be obtained during the drying sample. Moreover, the discovery of the minerals Ca- and Mg-phosphate allowed controlling the determination of the calcium content in the MAP solution, which influences the purity and productivity of struvite. This level of Ca concentration should be set in the actual wastewater by quantifying sufficient additional magnesium and potassium ions to compensate for the calcium concentration, which enables struvite and struvite-(K) to be produced at an economic value (Li et al., 2016; Yan & Shih, 2016).

3.4. Main findings of the present study

A stirred-batch lab of MAP crystallization under varying Ca/Mg ratio and pH solution was successfully demonstrated in the study, in which the kinetics of crystal growth for struvite and struvite-(K) as phosphate minerals that often generate a tenacious scale of industrial equipment. This study established the kinetic model representing curves of the pH changes versus the Mg^{2+} sensitivity under various experimental conditions. The kinetic analysis was focused on calculating rates of mineralization reactions and validating kinetic equations accordingly. Moreover, the crystallization rate of solid phase products could be derived from two reaction stages, including a severe initial pH reduction, accompanied by a gradual pH reduction until the end of the experiments. In the reaction process, the crystallisation kinetics of the precipitates obeyed two stages according to the pH reduction in the time periods of 0–3 min and 3–60 min, whereas both patterns appropriately fit the first-order kinetics.

In the case of minute Ca^{2+} amounts (1, 10, and 20 ppm) present in the MAP aqueous solution, faster solid-phase growth rates could be observed in both time periods that might be related to the crystal growth rates of struvite and struvite-(K) crystals, according to the XRPD Rietveld analysis (Table 3). However, growth rates dropped steadily as higher Ca concentrations were added (Ca/Mg molar ratio > 0.5). As a result, this condition increased the number of minerals that decreased growth rates. Additionally, the morphology of solid precipitation products was greatly changed. Therefore, this kinetic relationship provided a theoretical basis for the struvite and struvite-(K) crystal production with desired morphology. In fact, a significant effect on crystal morphology and structure developed during experiments might be contributed by the difference in crystal growth of Ca- and Mg-phosphate-bearing minerals.

Further investigation by the quantitative XRPD Rietveld analysis (Table 3) supported the previous finding in the literature that the competition of Ca-P and Mg-P promoted many minerals (e.g., hydroxyapatite, dolomite, Mg-whitlockite, and Newberyite) grew simultaneously during struvite crystallization (Xiaoning Liu & Wang, 2019; Yan & Shih, 2016), in which interfering of Ca made obstruction of the struvite crystallization. The rationale for the crystal growth for hydroxyapatite found in the study might be related to the nucleation of Ca-P easier than the MgP nucleation because of its lower solubility (Xiaoning Liu & Wang, 2019). For this reason, hydroxyapatite is more likely to precipitate preferentially rather than struvite at a higher Ca/Mg ratio (~2). Correspondingly,

an approach of controlling Ca/Mg ratio ions present in the MAP solution should be adopted for keeping a minimum level of these ions to enhance the struvite crystallization (Xiaoning Liu & Wang, 2019).

4. Conclusion

Struvite and struvite-(K) could be crystallized to recover phosphate, ammonium, and potassium levels in the presence of Ca-ion, which is common in wastewater. In this study, the impact of calcium ions on crystallization kinetics, mineralogical phases, and morphology were examined by analytical techniques. Overall, the crystallization kinetics of minerals from the aqueous solution included two stages according to the pH reduction: a severe initial reduction, accompanied by a gradual reduction until the end, in which growth rates could be derived from equations fit with first-order kinetics. Struvite and struvite-(K) crystallization rates were faster by Ca^{2+} ions present at limited doses (from 1 to 20 ppm). At the first stage, however, a gradual increased in the rate constants was observed with increasing Ca doses added to Ca/Mg > 0.5, while the second stages showed the gradual reduction of crystal growth rate. The quantitative XRPD analysis confirmed that lower concentrations of Ca (<20 ppm) did not influence the struvite and struvite-(K) crystallization. However, its adverse impact was evident with the increase Ca/Mg molar ratio to 0.5, which corresponds to the formation of Ca and Mg phosphates. Specifically, hydroxyapatite in terms of amorphous and crystalline phases was proposed to dominantly precipitate from the solution under higher Ca/Mg ratios (>0.5). For samples at Ca/Mg molar ratios of 1 and 0.5, the amount of hydroxyapatite was comparable with the quantity of struvite and struvite (K). but its amount became a major phase at Ca/Mg molar ratio of 2 along with the formation of Mg-whitlockite and newberyite. The struvite crystal with needle morphology could be observed at a higher Ca/Mg ratio, but in the subsequent decrease in Ca/Mg ratio, this morphology changed to an irregular shape. Further studies should focus on the control of calcium and magnesium in solutions at a low proportion for recovering phosphate and potassium from waste streams in order to produce the high quality and quantity of struvite and struvite-(K).

Author details
D. S. Perwitasari[1]
S. Muryanto[2]
mari[3]
ID ID: http://orcid.org/0000-0002-6172-2635
A. P. Bayuseno
E-mail: apbayuseno@lecturer.undip.ac.id
ORCID ID: http://orcid.org/0000-0002-0882-4480
ey Arellano-GarciaReviewing editor
[1] Department of Chemical Engineering, Universitas Pembangunan National "Veteran" Jawa Timur, Surabaya 60294 Indonesia.
[2] Department of Chemical Engineering UNTAG University in Semarang, Bendhan Dhuwur Campus, Semarang 50233, Indonesia.
[3] Centre for Waste Management, Department of Mechanical Engineering, Diponegoro University, Tembalang Campus, Semarang 50275, Indonesia.

Disclosure statement
No potential conflict of interest was reported by the authors.

Author Contributions
M.S. and B.A.P. designed the experiments. P.D.S and J.J prepared the solution and carried out crystallization experiments. B.A.P carried out Rietveld analysis of XRD data. P.D.S. carried out SEM and EDX studies. M.S; J.J and B.A.P. prepared and finally approved for the version to be published the manuscript.

References
Abbona, F., & Boistelle, R. (1979). Growth morphology and crystal habit of struvite crystals ($MgNH_4PO_4\cdot6\ H_2O$). *Journal of Crystal Growth, 46*(3), 339–354. https://doi.org/10.1016/0022-0248(79)90082-4

Abbona, F., Lundager Madsen, H. E., & Boistelle, R. (1988). The final phases of calcium and magnesium phosphates precipitated from solutions of high to medium concentration. *Journal of Crystal Growth, 89*(4), 592–602. https://doi.org/10.1016/0022-0248(88)90223-0

Abbona, F., Madsen, H. E. L., & Boistelle, R. (1986). The initial phases of calcium and magnesium phosphates precipitated from solutions of high to medium concentrations. *Journal of Crystal Growth, 74*(3), 581–590. https://doi.org/10.1016/0022-0248(86)90205-8

Ali, M. I., & Schneider, P. A. (2005). Crystallization of struvite from metastable region with different types of seed crystals. *Journal of Non-Equilibrium Thermodynamics, 30*(2), 95–111. https://doi.org/10.1515/JNETDY.2005.007

Ali, M. I., & Schneider, P. A. (2006). A fed-batch design approach of struvite precipitation in controlled supersaturation. *Chemical Engineering Science, 61*(12), 3951–3961. https://doi.org/10.1016/j.ces.2006.01.028

Bayuseno, A. P., Perwitasari, D. S., Muryanto, S., Tauviqirrahman, M., & Jamari, J. (2020). Kinetics and morphological characteristics of struvite ($MgNH_4PO_4 \cdot 6H_2O$) under the influence of maleic acid. *Heliyon, 6*(3), e03533. https://doi.org/10.1016/j.heliyon.2020.e03533

Bayuseno, A. P., & Schmahl, W. W. (2015). Improved understanding of the pozzolanic behaviour of MSWI fly ash with Ca(OH)₂ solution. *International Journal of Environment and Waste Management, 15*(1), 39–66. https://doi.org/10.1504/IJEWM.2015.066950

Bayuseno, A. P., & Schmahl, W. W. (2018). Hydrothermal synthesis of struvite and its phase transition: Impacts of pH, heating and subsequent cooling methods. *Journal of Crystal Growth, 4981*, 336–345 . https://doi.org/10.1016/j.jcrysgro.2018.06.026

Bayuseno, A. P., & Schmahl, W. W. (2020). Crystallization of struvite in a hydrothermal solution with and without calcium and carbonate ions. *Chemosphere, 250*(11), 126245. https://doi.org/10.1016/j.chemosphere.2020.126245

Bhuiyan, M. I. H., Mavinic, D. S., & Beckie, R. D. (2007). A solubility and thermodynamic study of struvite. *Environmental Technology, 28*(9), 1015–1026. https://doi.org/10.1080/09593332808618857

Bhuiyan, M. I. H., Mavinic, D. S., & Koch, F. A. (2008a). Thermal decomposition of struvite and its phase transition. *Chemosphere, 70*(8), 1347–1356. https://doi.org/10.1016/j.chemosphere.2007.09.056

Bhuiyan, M. I. H., Mavinic, D. S., & Koch, F. A. (2008b). Phosphorus recovery from wastewater through struvite formation in fluidized bed reactor: A sustainable approach. *Water Science and Technology, 57*(2), 175–181. https://doi.org/10.2166/wst.2008.002

Bouropoulos, N. C., & Koutsoukos, P. G. (2000). Spontaneous precipitation of struvite from aqueous solutions. *Journal of Crystal Growth, 213*(3–4), 381–388. https://doi.org/10.1016/S0022-0248(00)00351-1

Capdevielle, A., Sykorova, E., Biscans, B., Beline, F., & Daumer, M. L. (2013). Optimization of struvite precipitation in synthetic biologically treated swine wastewater – Determination of the optimal process parameters. *Journal of Hazardous Materials, 244*(15), 357–369. https://doi.org/10.1016/j.jhazmat.2012.11.054

Çelen, I., Buchanan, J. R., Burns, R. T., Robinson, R. B., & Raman, D. R. (2007). Using a chemical equilibrium model to predict amendments required to precipitate phosphorus as struvite in liquid swine manure. *Water Research, 41*(8), 1689–1696. https://doi.org/10.1016/j.watres.2007.01.018

Crutchik, D., & Garrido, J. M. (2011). Struvite crystallization versus amorphous magnesium and calcium phosphate precipitation during the treatment of a saline industrial wastewater. *Water Science and Technology, 64*(12), 2460–2467. https://doi.org/10.2166/wst.2011.836

Dalecha, T., Assefa, E., Krasteva, K., & Meinhold, K. (2014). Struvite production from source separated urine: Application and economic feasibility in Arba Minch, Ethiopia. *Sustainable Sanitation Practice, 19*(4), 16–22. http://doi.org/10.3390/SU3031363

Darwish, M., Aris, A., Puteh, M. H., Jusoh, M. N. H., & Kadir, A. A. (2017). Waste bones ash as an alternative source of P for struvite precipitation. *Journal of Environmental Management, 203*(2), 861–866. https://doi.org/10.1016/j.jenvman.2016.02.033

Desmidt, E., Ghyselbrecht, K., Monballiu, A., Rabaey, K., Verstraete, W., & Meesschaert, B. D. (2013). Factors influencing urease driven struvite precipitation. *Separation and Purification Technology, 110*(7), 150–157. https://doi.org/10.1016/j.seppur.2013.03.010

Downs, R. T., & Hall-Wallace, M. (2003). The American mineralogist crystal structure database. *American Mineralogist, 88*(1), 247–250. http://doi.org/10.5408/089-995-52.1.76

Doyle, J. D., & Parsons, S. A. (2002). Struvite formation, control and recovery. *Water Research, 36*(16), 3925–3940. https://doi.org/10.1016/S0043-1354(02)00126-4

Guillen-Jimenez, E., Alvarez-Mateos, P., Romero-Guzman, F., Pereda-Marin, F., Hao, X., Wang, C., van Loosdrecht, M. C. M., & Hu, Y. (2000). Bio-mineralization of organic matter in dairy wastewater, as affected by pH. The evolution of ammonium and phosphates. *Water Research, 34*(4), 1215–1224. https://doi.org/10.1016/S0043-1354(99)00290-0

Gunay, A., Karadag, D., Tosun, I., & Ozturk, A. (2008). Use of magnesit as a magnesium source for ammonium removal from leachate. *Journal of Hazardous Materials, 156*(1–3), 619–623. https://doi.org/10.1016/j.jhazmat.2007.12.067

Hao, X., Wang, C., Van Loosdrecht, M. C. M., & Hu, Y. (2013). Looking beyond struvite for P-recovery. *Environmental Science & Technology, 47*(10), 4965–4966. https://doi.org/10.1021/es401140s

Hill, R. J., & Howard, C. J. (1987). Quantitative phase analysis from neutron powder diffraction data using the Rietveld method. *Journal of Applied Crystallography, 20*(6), 467–474. https://doi.org/10.1107/S0021889887086199

Huang, A. H., & Liu, J. C. (2014). Removal of ammonium as struvite from wet scrubber wastewater. *Water, Air, & Soil Pollution, 225*(8), 1–9. https://doi.org/10.1007/s11270-014-2062-2

Huang, H. M., Zhang, D. D., Wang, W. J., Li, B., Zhao, N., Li, J., & Dai, J. K. (2019). Alleviating Na⁺ effect on phosphate and potassium recovery from synthetic urine by K struvite crystallization using different magnesium sources. *Science of the Total Environment, 655*(10), 211–219. https://doi.org/10.1016/j.scitotenv.2018.11.259

Huchzermeier, M. P., & Tao, W. (2012). Overcoming challenges to struvite recovery from anaerobically digested dairy manure. *Water Environment Research, 84*(1), 34–41. https://doi.org/10.2175/106143011X13183708018887

Karabegovic, L., Uldal, M., Werker, A., & Morgan-Sagastume, F. (2013). Phosphorus recovery potential from a waste stream with high organic and nutrient contents via struvite precipitation. *Environmental Technology, 34*(7), 871–883. https://doi.org/10.1080/09593330.2012.720718

Kofina, A. N., Demadis, K. D., & Koutsoukos, P. G. (2007). The effect of citrate and phosphocitrate on struvite spontaneous precipitation. *Crystal Growth & Design, 7*(12), 2705–2712. https://doi.org/10.1021/cg0603927

Kontrec, J., Babić-Ivančić, V., & Brecević, L. (2005). Formation and Morphology of struvite and newberyite in aqueous solutions at 25 and 37 °C. *Collegium antropologicum, 29*(1), 289–294.

Lagier, R., & Baud, C.-A. (2003). Magnesium whitlockite, a calcium phosphate crystal of special interest in Pathology. *Pathology Research and Practice, 199*(5), 329–335 http://doi.org/0.1078/0344-0338-00425

Lahav, O., Telzhensky, M., Zewuhn, A., Gendel, Y., Gerth, J., Calmano, W., & Birnhack, L. (2013). Struvite recovery from municipal-wastewater sludge centrifuge supernatant using seawater NF concentrate as a cheap Mg(II) source. *Separation and Purification Technology, 108*(4), 103–110. https://doi.org/10.1016/j.seppur.2013.02.002

Le Corre, K. S., Understanding Struvite Crystallization and Recovery. PhD thesis, Cranfield University. 2006, 72–73.

Le Corre, K. S., Valsami-Jones, E., Hobbs, P., & Parsons, S. A. (2005). Impact of calcium on struvite crystal size,

shape and purity. *Journal of Crystal Growth, 283*(3–4), 514–522. https://doi.org/10.1016/j.jcrysgro.2005.06.012

Le Corre, K. S., Valsami-Jones, E., Hobbs, P., & Parsons, S. A. (2009). Phosphorus recovery from wastewater by struvite crystallization: A review. *Critical Reviews in Environmental Science and Technology, 39*(6), 433–477. https://doi.org/10.1080/10643380701640573

Lee, S.-H., Yoo, B.-H., Lim, S. J., Kim, T.-H., Kim, S.-K., & Kim, J. Y. (2013). Development and validation of an equilibrium model for struvite formation with calcium coprecipitation. *Journal of Crystal Growth, 372*(6), 129–137. https://doi.org/10.1016/j.jcrysgro.2013.03.010

Li, B., Boiarkina, I., Young, B., & Yu, W. (2016). Quantification and mitigation of the negative impact of calcium on struvite purity. *Advanced Powder Technology, 27*(6), 2354–2362. https://doi.org/10.1016/j.apt.2016.10.003

Li, B., Boiarkina, I, Yu, W., Huang, H., Munir, T., Wang, G., & Young, B. (2019). Phosphorous recovery through struvite crystallization: Challenges for future design. *Science of the Total Environment, 648*(1), 1244–1256. https://doi.org/10.1016/j.scitotenv.2018.07.166

Liu, Y., Kumar, S., Kwag, J. H., & Ra, C. (2013). Magnesium ammonium phosphate formation, recovery and its application as valuable resources: A review. *Journal of Chemical Technology & Biotechnology, 88*(2), 181–189. https://doi.org/10.1002/jctb.3936

Mahieux, P.-Y., Aubert, J.-E., Cyr, M., Coutand, M., & Husson, B. (2010). Quantitative mineralogical composition of complex mineral wastes–contribution of the Rietveld method. *Waste Manage, 30*(3), 378–388 http://doi.org/10.1016/j.wasman.2009.10.023

Muryanto, S., & Bayuseno, A. P. (2014). Influence of Cu^{2+} and Zn^{2+} as additives on crystallization kinetics and morphology of struvite. *Powder Technology, 253*(2), 602–607. https://doi.org/10.1016/j.powtec.2013.12.027

Nelson, N. O., Mikkelsen, R. L., & Hesterberg, D. L. (2003). Struvite precipitation in anaerobic swine lagoon liquid: Effect of pH and Mg: P ratio and determination of rate constant. *Bioresource Technology, 89*(3), 229–236. https://doi.org/10.1016/S0960-8524(03)00076-2

Pastor, L., Mangin, D., Barat, R., & Seco, A. (2008). A pilot-scale study of struvite precipitation in a stirred tank reactor: Conditions influencing the process. *Bioresource Technology, 99*(14), 6285–6291. https://doi.org/10.1016/j.biortech.2007.12.003

Prywer, J., Torzewska, A., & Plocinski, T. (2012). Unique surface and internal structure of struvite crystals formed by Proteus mirabilis. *Urological Research, 40*(6), 699–707. https://doi.org/10.1007/s00240-012-0501-3

Quintana, M., Sanchez, E., Colmenarejo, M. F., Barrera, J., Garcia, G., & Borja, R. (2005). Kinetics of phosphorus removal and struvite formation by the utilization of by-product of magnesium oxide production. *Chemical Engineering Journal, 111*(1), 45–52. https://doi.org/10.1016/j.cej.2005.05.005

Rahaman, M. S., Mavinic, D. S., & Ellis, N. (2008). Effects of various process parameters on struvite precipitation kinetics and subsequent determination of rate constants. *Water Science and Technology, 57*(5), 647–654. https://doi.org/10.2166/wst.2008.022

Rahman, M. M., Liu, Y. H., Kwag, J. H., & Ra, C. S. (2011). Recovery of struvite from animal wastewater and its nutrient leaching loss in soil. *Journal of Hazardous Materials, 2011*(2–3), 2026–2030. http://doi.org/10.1016/j.jhazmat.2010.12.103

Rodriguez-Carvajal, J. (June 2005). Program Fullprof.2k, version 3.30, Laboratoire Leon Brillouin, France.

Sabbag, H., Lerner, A., Nikolski, A., & Borojovich, E. J. C. (2015). Prevention and control of struvite and calcium phosphate precipitation by chelating agents. *Desalination and Water Treatment, 55*(1), 61–69. https://doi.org/10.1080/19443994.2014.910840

Scholz, R. W., Ulrich, A. E., Eilittä, M., & Roy, A. (2013). Sustainable use of phosphorus: A finite resource. *Science of the Total Environment, 461*(9), 799–803. https://doi.org/10.1016/j.scitotenv.2013.05.043

Shih, Y. J., Abara, R. R. M., de Luna, M. D. G., Huang, Y. H., & Lu, M. C. (2017). Recovery of phosphorus from synthetic wastewaters by struvite crystallization in a fluidized-bed reactor: Effects of pH, phosphate concentration and coexisting ions. *Chemosphere, 173*(4), 466–473. https://doi.org/10.1016/j.chemosphere.2017.01.088

Song, Y., Dai, Y., Hu, Q., Yu, X., & Qian, F. (2014). Effects of three kinds of organic acids on phosphorus recovery by magnesium ammonium phosphate (MAP) crystallization from synthetic swine wastewater. *Chemosphere, 101*(4), 41–48. https://doi.org/10.1016/j.chemosphere.2013.11.019

Song, Y. H., Donnert, D., Berg, U., Weidler, P. G., & Nueesch, R. (2007). Seed selections for crystallization of calcium phosphate for phosphorus recovery. *Journal of Environmental Sciences, 19*(5), 591–595. https://doi.org/10.1016/S1001-0742(07)60098-9

Song, Y. H., Yuan, P., Zheng, B. H., Peng, J. F., Yuan, F., & Gao, Y. (2007). Nutrients removal and recovery by crystallization of magnesium ammonium phosphate from synthetic swine wastewater. *Chemosphere, 69*(2), 319–324. https://doi.org/10.1016/j.chemosphere.2007.06.001

Wang, J., Burken, J. G., Zhang, X., & Surampalli, R. (2005). Engineered struvite precipitation: Impacts of component-ion molar ratios and pH. *Journal of Environmental Engineering, 131*(10), 1433–1440. https://doi.org/10.1061/(ASCE)0733-9372(2005)131:10(1433)

Wiles, D. T., & Young, R. (1981). A new computer program for Rietveld analysis of X-ray powder diffraction patterns. *Journal of Applied Crystallography, 14*(2), 149–151. https://doi.org/10.1107/S0021889881008996

Xiaoning Liu, X., & Wang, J. (2019). Impact of calcium on struvite crystallization in the wastewater and its competition with magnesium. *Chemical Engineering Journal, 378*(12), 122121. https://doi.org/10.1016/j.cej.2019.122121

Yan, H., & Shih, K. (2016). Effects of calcium and ferric ions on struvite precipitation: A new assessment based on quantitative X-ray diffraction analysis. *Water Research, 95*(5), 310–318. https://doi.org/10.1016/j.watres.2016.03.032

Young, R. (1993). *The Rietveld method, IUCr. Monographs on crystallography.* Oxford University Press.

cogent • engineering

Cogent Engineering (ISSN: 2331-1916) is published by Cogent OA, part of Taylor & Francis Group.

Publishing with Cogent OA ensures:

- Immediate, universal access to your article on publication
- High visibility and discoverability via the Cogent OA website as well as Taylor & Francis Online
- Download and citation statistics for your article
- Rapid online publication
- Input from, and dialog with, expert editors and editorial boards
- Retention of full copyright of your article
- Guaranteed legacy preservation of your article
- Discounts and waivers for authors in developing regions

Submit your manuscript to a Cogent OA journal at www.CogentOA.com

Crystallization of struvite in the presence of calcium ions: Change in reaction rate, morphology and chemical composition

NUTRIENT RECOVERY IN WASTEWATER TREATMENT", International Journal of Energy for a Clean Environment, 2021
Publication

9	**p3.snf.ch** Internet Source	<1%
10	**repository.unusa.ac.id** Internet Source	<1%
11	**ijme.iranjournals.ir** Internet Source	<1%
12	**www.iapjournals.ac.cn** Internet Source	<1%
13	**www.ncbi.nlm.nih.gov** Internet Source	<1%
14	**nemertes.lis.upatras.gr** Internet Source	<1%
15	**www.iue.cas.cn** Internet Source	<1%
16	**Cusick, R.D.. "Phosphate recovery as struvite within a single chamber microbial electrolysis cell", Bioresource Technology, 201203** Publication	<1%
17	**psenterprise.com** Internet Source	<1%

18 E. Todd Howell, G. Robin South. " Population dynamics of (Chlorophyta, Desmidiaceae) in relation to a minerotrophic gradient on a Newfoundland fen ", British Phycological Journal, 2007
Publication
<1%

19 dl.icdst.org
Internet Source
<1%

20 jurnal.untag-sby.ac.id
Internet Source
<1%

21 scholarworks.uvm.edu
Internet Source
<1%

22 d-scholarship.pitt.edu
Internet Source
<1%

23 sites.google.com
Internet Source
<1%

24 www.esf.edu
Internet Source
<1%

25 Le Corre, K.S.. "Impact of calcium on struvite crystal size, shape and purity", Journal of Crystal Growth, 20051001
Publication
<1%

26 library.naturalsciences.be
Internet Source
<1%

27 ijstr.org
Internet Source

<1 %

| 28 | opac.elte.hu
Internet Source | <1 % |

| 29 | profiles.arizona.edu
Internet Source | <1 % |

| 30 | structurae.net
Internet Source | <1 % |

| 31 | minerva-access.unimelb.edu.au
Internet Source | <1 % |

| 32 | www.investigacion.us.es
Internet Source | <1 % |

| 33 | kups.ub.uni-koeln.de
Internet Source | <1 % |

| 34 | uknowledge.uky.edu
Internet Source | <1 % |

| 35 | www.nstproceeding.com
Internet Source | <1 % |

| 36 | Xiaoyun Wu, Rongrong Xie, Jianguo Ding, Liping Dai et al. "Recovery of phosphate and ammonium nitrogen as struvite from aqueous solutions using a magnesium–air cell system", Science of The Total Environment, 2022
Publication | <1 % |

engineering.utm.my

| 37 | Internet Source | <1% |

| 38 | ccp14.sims.nrc.ca
Internet Source | <1% |

| 39 | patents.google.com
Internet Source | <1% |

| 40 | Mohamad Djaeni, Hadiyanto Hadiyanto, Andri Cahyo Kumoro, Febiani Dwi Utari, Ching-Lik Hii. "Improvements in thermal efficiency of onion slice drying by exhaust air recycling", Cogent Engineering, 2021
Publication | <1% |

| 41 | libmast.utm.my
Internet Source | <1% |

| 42 | netl.doe.gov
Internet Source | <1% |

| 43 | www.iucr.org
Internet Source | <1% |

| 44 | jeatdisord.biomedcentral.com
Internet Source | <1% |

| 45 | researchspace.ukzn.ac.za
Internet Source | <1% |

| 46 | W. D. Lestari, D. K. Nababan, R. Ismail, J. Jamari, Athanasius P. Bayuseno. "Dimensional Accuracy and Surface Roughness of | <1% |

Acetabular Liner with UHMWPE: Assessment Results between Compression Molding and CNC Milling", International Review of Mechanical Engineering (IREME), 2018
Publication

47 cris.vtt.fi
Internet Source
<1%

48 epdf.pub
Internet Source
<1%

49 www.miniweb.com.br
Internet Source
<1%

50 www.termedia.pl
Internet Source
<1%

51 Anuraag Bukkuri. "On the Contribution of Reproductive and Offspring Investment on Fertility: Human and Animal Societies", Cold Spring Harbor Laboratory, 2021
Publication
<1%

52 ena.lp.edu.ua:8080
Internet Source
<1%

53 jnanobiotechnology.biomedcentral.com
Internet Source
<1%

54 www.itobiad.com
Internet Source
<1%

55 August Bonmatí-Blasi, Míriam Cerrillo-Moreno, Victor Riau-Arenas. "chapter 3
<1%

Systems Based on Physical-Chemical Processes", IGI Global, 2017
Publication

56 Muster, T.H., G.B. Douglas, N. Sherman, A. Seeber, N. Wright, and Y. Güzükara. "Towards effective phosphorus recycling from wastewater: Quantity and quality", Chemosphere, 2013.
Publication

<1%

<1%

57 bibl.vgltu.ru
Internet Source

<1%

58 cherry.chem.bg.ac.rs
Internet Source

<1%

59 childandfamilysuccess.asu.edu
Internet Source

<1%

60 dr.ntu.edu.sg
Internet Source

<1%

61 ejournal2.undip.ac.id
Internet Source

<1%

62 lsmll.journals.umcs.pl
Internet Source

<1%

63 researchwith.montclair.edu
Internet Source

<1%

64 scholars.ncu.edu.tw
Internet Source

<1%

65 temp1.auinstallation32.cs.au.dk
Internet Source
<1%

66 wellcomeopenresearch.org
Internet Source
<1%

67 worldwidescience.org
Internet Source
<1%

68 wrap.warwick.ac.uk
Internet Source
<1%

69 www.asprs.org
Internet Source
<1%

70 www.chbe.ubc.ca
Internet Source
<1%

71 www.fordham.edu
Internet Source
<1%

72 www.ijraset.com
Internet Source
<1%

73 www.neliti.com
Internet Source
<1%

74 "Phosphorus Recovery and Recycling", Springer Science and Business Media LLC, 2019
Publication
<1%

75 Dyah Suci Perwitasari, Sintha Soraya Santi, Stefanus Muryanto, J Jamari, AP Bayuseno.
<1%

"Study of Struvite Crystal Growth with The Addition of Tartaric Acid", E3S Web of Conferences, 2021
Publication

76 Rifky Ismail, Dewi Paras Utami, Mochamad Arid Irfai, J. Jamari, A.P. Bayuseno. "Mechanical properties of Carbon-matrix composites for a blade runner's artificial leg", Cogent Engineering, 2021
Publication

<1 %

77 aflasafe.com
Internet Source

<1 %

78 authors.library.caltech.edu
Internet Source

<1 %

79 es.scribd.com
Internet Source

<1 %

80 health.hawaii.gov
Internet Source

<1 %

81 ir.fy.edu.tw:8080
Internet Source

<1 %

82 onepetro.org
Internet Source

<1 %

83 refubium.fu-berlin.de
Internet Source

<1 %

84 reprints.hindawi.com
Internet Source

<1 %

85 sustinerejes.com
Internet Source
<1 %

86 uluslararasi.mersin.edu.tr
Internet Source
<1 %

87 www.businessperspectives.org
Internet Source
<1 %

88 Haiming Huang, DingDing Zhang, Jing Li, Guojun Guo, Shoufeng Tang. "Phosphate recovery from swine wastewater using plant ash in chemical crystallization", Journal of Cleaner Production, 2017
Publication
<1 %

89 Tao, Wendong, Kazi P. Fattah, and Matthew P. Huchzermeier. "Struvite recovery from anaerobically digested dairy manure: A review of application potential and hindrances", Journal of Environmental Management, 2016.
Publication
<1 %

90 Gray, . "BACK MATTER", Series on Environmental Science and Management, 2004.
Publication
<1 %

91 Guanglei Qiu, Yi-Ming Law, Subhabrata Das, Yen-Peng Ting. "Direct and Complete Phosphorus Recovery from Municipal Wastewater Using a Hybrid Microfiltration-Forward Osmosis Membrane Bioreactor
<1 %

Process with Seawater Brine as Draw Solution", Environmental Science & Technology, 2015
Publication

92   Hui Lin, Yun Chen, Nan Shen, Yang Deng, Wang Yan, Roby Ruhyadi, Guoxiang Wang. "Effects of individual volatile fatty acids (VFAs) on phosphorus recovery by magnesium ammonium phosphate", Environmental Pollution, 2020
Publication   <1 %

93   Paulus Wisnu Anggoro, M. Tauviqirrahman, J. Jamari, A. P. Bayuseno, B. Bawono, M. M. Avelina. "Computer-aided reverse engineering system in the design and production of orthotic insole shoes for patients with diabetes", Cogent Engineering, 2018
Publication   <1 %

| Exclude quotes | Off | Exclude matches | Off |
| Exclude bibliography | Off | | |